

Annual Technical Report

**Research Related to the Development, Fabrication and
Characterization of UV Detectors and Cold Cathode Devices**

Supported under Grant #N00014-96-1-0765
Office of the Chief of Naval Research
Report for the period 1/1/98-12/31/98

R. F. Davis, E. Carlson, T. Gehrke, A. D. Hanser,
P. Hartlieb, K. Linthicum, W. G. Perry, P. Rajagopal,
C. Ronning, D. B. Thomson, and T. S. Zheleva
North Carolina State University
Materials Science and Engineering Department
Campus Box 7907
Raleigh, NC 27695

19990122 095

December, 1998

REPORT DOCUMENTATION PAGE

Form Approved
OMB No. 0704-0188

Public reporting burden for this collection of information is estimated to average 1 hour per response, including the time for reviewing instructions, searching existing data sources, gathering and maintaining the data needed, and completing and reviewing the collection of information. Send comments regarding this burden estimate or any other aspect of this collection of information, including suggestions for reducing this burden to Washington Headquarters Services, Directorate for Information Operations and Reports, 1215 Jefferson Davis Highway, Suite 1204, Arlington, VA 22202-4302, and to the Office of Management and Budget Paperwork Reduction Project (0704-0188), Washington, DC 20503.

1. AGENCY USE ONLY (Leave blank)

2. REPORT DATE

December, 1998

3. REPORT TYPE AND DATES COVERED

Annual Technical 1/1/98-12/31/98

4. TITLE AND SUBTITLE

Research Related to the Development, Fabrication and Characterization of UV Detectors and Cold Cathode Devices

5. FUNDING NUMBERS

s400003srr14
1114SS
N00179
N66005
4B855

6. AUTHOR(S)

R. F. Davis

7. PERFORMING ORGANIZATION NAME(S) AND ADDRESS(ES)

North Carolina State University
Hillsborough Street
Raleigh, NC 27695

8. PERFORMING ORGANIZATION
REPORT NUMBER

N00014-96-1-0765

9. SPONSORING/MONITORING AGENCY NAMES(S) AND ADDRESS(ES)

Sponsoring: ONR, Code 312, 800 N. Quincy, Arlington, VA 22217-5660
Monitoring: Admin. Contracting Officer, ONR, Regional Office Atlanta
101 Marietta Tower, Suite 2805
101 Marietta Street
Atlanta, GA 30323-0008

10. SPONSORING/MONITORING
AGENCY REPORT NUMBER

11. SUPPLEMENTARY NOTES

12a. DISTRIBUTION/AVAILABILITY STATEMENT

Approved for Public Release; Distribution Unlimited

12b. DISTRIBUTION CODE

13. ABSTRACT (Maximum 200 words)

Pendeo-epitaxial growth of GaN films has been investigated as a function of growth temperature on etched, elongated GaN seed columns grown on AlN/6H-SiC (0001) substrates via metalorganic vapor phase epitaxy (MOVPE). Silicon nitride mask layers atop the GaN seed columns forced growth from the sidewalls of the columns. Higher growth temperatures resulted in improved coalescence due to greater lateral-to-vertical growth ratios. Thin films of AlN and GaN were also deposited via conventional approaches on $\alpha(6H)$ -SiC(0001) wafers using H_2 and N_2 diluents. A computational fluid dynamic model of the deposition process was used to analyze the film growth conditions for both diluents. Low temperature (12 K) photoluminescence of the GaN films grown in N_2 had peak intensities and full widths at half maximum of ~ 7 meV which were equal to or better than those films grown in H_2 . Cross-sectional and plan view transmission electron microscopy of GaN films grown in both diluents showed similar microstructures with a typical dislocation density of $10^9/cm^2$. Hall measurements of n-type (Si doped) GaN grown in N_2 revealed Hall mobilities equivalent to those films grown in H_2 . Acceptor-type behavior of Mg-doped GaN grown in N_2 was repeatedly obtained without post-growth annealing. Secondary ion mass spectrometry revealed equivalent levels of H in Mg-doped GaN films grown in both diluents. The electrical properties of Ni/Au contacts on p-type, Mg-doped GaN films have been characterized using current-voltage measurements. Prior to the metallization, films with net ionized impurity concentrations of approximately $7 \times 10^{17} cm^{-3}$ and $2 \times 10^{17} cm^{-3}$ were heated to $990^\circ C$ and $800^\circ C$, respectively, and subsequently exposed to a 300 W atomic nitrogen plasma for 10 minutes. The contacts treated at $990^\circ C$ yielded the lowest specific contact resistivity, which was $50 \pm 7 \Omega \cdot cm^2$.

14. SUBJECT TERMS

pendeo-epitaxy, GaN, AlN, metalorganic vapor phase epitaxy, thin films, temperature, diluent, fluid dynamic, photoluminescence, transmission electron microscopy, microstructure, dislocation density, Hall mobility, secondary ion mass spectrometry, Mg, acceptor, ohmic contacts, p-type, current-voltage, metallization, specific contact resistivity, atomic nitrogen plasma

15. NUMBER OF PAGES

22

16. PRICE CODE

17. SECURITY CLASSIFICATION
OF REPORT

UNCLAS

18. SECURITY CLASSIFICATION
OF THIS PAGE

UNCLAS

19. SECURITY CLASSIFICATION
OF ABSTRACT

UNCLAS

20. LIMITATION OF ABSTRACT

SAR

Table of Contents

I.	Introduction	1
II.	Ranges of Deposition Temperatures Applicable for Metalorganic Vapor Phase Epitaxy of GaN Films Via the Technique of Pendeo-epitaxy <i>D. B. Thomson, T. Gehrke, K. J. Linthicum, P. Rajagopal, and R. F. Davis</i>	3
III.	Diluent Gas Effects on Properties of AlN and GaN Thin Films Grown by Metalorganic Vapor Phase Epitaxy on $\alpha(6H)$ -SiC Substrates <i>A. Hanser, C. Wolden, W. Perry, T. Zheleva, E. Carlson, P. Hartlieb and R. F. Davis</i>	9
IV.	Electrical Properties of Ni/Au Contacts Deposited on Plasma Treated p-GaN Films Grown Via Organometallic Vapor Phase Epitaxy <i>P. Hartlieb, K. Linthicum, C. Ronning, D. Thomson, and R. F. Davis</i>	17
V.	Distribution List	22

I. Introduction

The numerous potential semiconductor applications of the wide band gap III-nitrides has prompted significant research regarding their growth and development. Gallium nitride (wurtzite structure), the most studied in this group, has a bandgap of ≈ 3.4 eV and forms continuous solid solutions with both AlN (6.2 eV) and InN (1.9 eV). As such, materials with engineered band gaps are feasible for optoelectronic devices tunable in wavelength from the visible to the deep UV. The relatively strong atomic bonding of these materials also points to their application for high-power and high-temperature microelectronic devices. Diodes emitting light from the yellow into the blue regions of the spectrum, blue emitting lasers, and several types of high-frequency and high-power devices have recently been fabricated from these materials.

Single crystal wafers of GaN are not commercially available. Sapphire(0001) is the most commonly used substrate, although its lattice parameter and coefficients of thermal expansion are significantly different from that of any III-nitride. The heteroepitaxial nucleation and growth of monocrystalline films of GaN on any substrate and AlN on sapphire are difficult at elevated ($>900^\circ\text{C}$) temperatures. Therefore, at present, for successful organometallic vapor phase epitaxy (OMVPE) of GaN films on sapphire, the use of the initial deposition of an amorphous or polycrystalline buffer layer of AlN [1,2] or GaN [3,4] at low-temperatures ($450^\circ\text{--}600^\circ\text{C}$) is necessary to achieve both nucleation and relatively uniform coverage of the substrate surface. Subsequent deposition at higher temperatures and concomitant grain orientation competition has resulted in films of GaN(0001) and various nitrides alloys of improved quality and surface morphology relative to that achieved by growth directly on this substrate.

By contrast, we have observed that AlN and $\text{Al}_x\text{Ga}_{1-x}\text{N}$ alloys containing even low ($x \geq 0.05$) concentrations of AlN deposited on 6H-SiC(0001) substrates at high ($\geq 1000^\circ\text{C}$) temperatures undergo two-dimensional nucleation and growth with resulting uniform surface coverage. In this research, the use of a 1000 Å, monocrystalline, high-temperature (1100°C) AlN buffer has resulted in GaN films void of oriented domain structures and associated low-angle grain boundaries [5,6]. Monocrystalline films of $\text{Al}_x\text{Ga}_{1-x}\text{N}$ ($0.05 \leq x \leq 0.70$) of the same quality have also been achieved at 1100°C .

The investigations to 1975 regarding III-Nitrides in terms of thin films growth, characterization, properties and device development have been reviewed by Kesamanly [7] and Pankove and Bloom [8]. The considerable progress accomplished in these areas in the intervening years has been reviewed in Refs. [9–16]. Research in the authors' group at NCSU employs both MOCVD and GSMBE to grow GaN and $\text{Al}_x\text{Ga}_{1-x}\text{N}$ films on $\alpha(6\text{H})\text{-SiC}(0001)_{\text{Si}}$ substrates. Only the investigations involving the former technique are described herein.

Selective growth of particular microstructures have been used extensively for the fabrication of semiconductor devices such as quantum well, wire and dot structures, as well as

field emitter structures. The selective growth of GaN and $\text{Al}_{0.1}\text{Ga}_{0.9}\text{N}$ linear windows and GaN hexagonal pyramid arrays on dot-patterned GaN/sapphire substrates have been reported [17,18]. The first field emission from an undoped GaN hexagonal pyramid array on a GaN/sapphire substrate has also been observed [18], and the enhancement of field emission performance was recently reported [20]. Thus far, all research regarding selective growth of GaN has used sapphire substrates. However, in the present research, 6H-SiC substrates have been employed with excellent results.

In this reporting period, research has been conducted in the following areas: (1) pendeo-epitaxial growth of GaN thin films as a function of temperature, (2) conventional metalorganic vapor phase epitaxy (MOVPE) of AlN and GaN thin films in H_2 and N_2 diluents with n(Si)- and p(Mg)-type doping and the characterization of these films via photoluminescence, transmission electron microscopy, Hall measurements, and secondary ion mass spectrometry, (3) computational fluid dynamic modeling of the MOVPE deposition process to analyze the film growth conditions for the films noted in (2), and determination of the electrical properties of Ni/Au contacts on p-type, Mg-doped GaN films as a function of heating and exposure to an atomic nitrogen plasma. The following sections are self-contained in that they provide an introduction, results, discussion of results, conclusions and references for a given topic.

References

1. M.A. Khan, J.N. Kuznia, D.T. Olson, and R. Kaplan, *J. Appl. Phys.* **73**, 3108 (1993).
2. H. Amano, I. Akasaki, K. Hiramatsu, N. Koide, and N. Sawaki, *Thin Solid Films* **163**, 415 (1988).
3. J. Kuznia, M. Khan, D. Olson, R. Kaplan and J. Freitas, *J. Appl. Phys.* **73**, 4700 (1993).
4. S. Nakamura, *Jpn. J. Appl. Phys.* **30**, L1705 (1991).
5. T.W. Weeks, M. Bremser, K. Ailey, E. Carlson, W. Perry, R. Davis, *Appl. Phys. Lett.* **67**, 401 (1995).
6. T.W. Weeks, Jr., M.D. Bremser, K.S. Ailey, W.G. Perry, E.P. Carlson, E.L. Piner, N. A. El-Masry, and R.F. Davis, *J. Mat. Res. J.* **11**, 1081 (1996).
7. F. P. Kesamanly, *Sov. Phys. Semicond.* **8**, 147 (1974).
8. J. I. Pankove and S. Bloom, *RCA Rev.* **36**, 163 (1975).
9. R. F. Davis, *et al.*, *J. Mater. Sci. Eng. B* **1**, 77 (1988).
10. S. Strite and H. Morkoc, *J. Vac. Sci. Technol. B* **10**, 1237 (1992).
11. J. I. Pankove, in *Diamond, Silicon Carbide and Related Wide Bandgap Semiconductor Materials*, edited by J. T. Glass, R. F. Messier, and N. Fujimori, (Mater. Res. Soc. Sym Proc. Vol. 116, Pittsburgh, PA, (1990), 515-524.
12. R. F. Davis, *Proc. IEEE* **79**, 702 (1991).
13. H. Morkoc, *et al.*, *J. Appl. Phys.* **76**, 1363 (1994).
14. J. H. Edgar, *J. Mater. Res.* **7**, 235 (1992).
15. M. Henin, *J. Microelectron.* **23**, 500 (1992).
16. H. Morkoc, S. Strite, G.B. Gao, M.E. Lin, B. Sverdlov, and M. Burns, *J. Appl Phys.* **76**, 1363 (1994).
17. S. Kitamura, K. Hiramatsu and N. Sawaki, *Jpn. J. Appl. Phys.* **34**, 2284 (1995).
18. R. D. Underwood, D. Kapolnek, B. P. Keller, S.Keller, S. P. DenBaars and U. K. Mishra, *Topical Workshop on Nitrides*, Nagoya, Japan, September (1995).
19. T. Tanaka, K. Uchida, A. Watanabe and S. Minagawa, *Appl. Phys. Lett.* **68**, 976 (1996).

II. Ranges of Deposition Temperatures Applicable for Metalorganic Vapor Phase Epitaxy of GaN Films Via the Technique of Pendeo-epitaxy

D. B. Thomson, T. Gehrke, K. J. Linthicum, P. Rajagopal, and R. F. Davis
Department of Materials Science and Engineering, North Carolina State University, Box 7907,
Raleigh, NC 27695-7907

Abstract

Pendeo-epitaxy is a type of selective growth of thin films from the sidewalls of etched forms. The resulting films are suspended from the sidewalls and do not interface with the substrate. In this research, pendeo-epitaxial growth of GaN films has been achieved on elongated GaN seed columns. The seed columns were etched from GaN grown on 6H-SiC (0001) substrates via metalorganic vapor phase epitaxy (MOVPE). Silicon nitride mask layers on top of the GaN seed columns forced growth from the sidewalls. Pendeo-epitaxial growth of GaN was investigated using several growth temperatures. Higher growth temperatures resulted in improved coalescence due to greater lateral to vertical growth ratios.

A. Introduction

The III-Nitride community has shown considerable interest in the technique of lateral epitaxial overgrowth (LEO) of GaN and related materials. This interest was boosted by the report of Nakamura *et al.* [1] of a projected laser diode lifetime of 10,000 hours in GaN-based devices fabricated using LEO. In conventional lateral epitaxy, GaN initially grows vertically within the openings of a patterned mask layer. Lateral growth of this material from these openings and over the masked areas results when the proper process parameters are employed. Transmission electron microscopy has shown that the masked areas stop the propagation of threading dislocations which arise from lattice mismatch at the GaN/AlN and AlN/6H-SiC interfaces. As such, the overgrown GaN regions contain four-to-six orders of magnitude lower density of dislocations relative to the unmasked regions [2].

Conventional single layer LEO films consist of alternating lateral regions of high and low defect density GaN. Device placement requires careful alignment with respect to the underlying mask stripes to take advantage of the superior quality material. Device size is limited to the width of the mask stripes. It is, therefore, desirable to have a continuous layer of low defect material over the entire GaN surface such that devices can be fabricated anywhere on the wafer without confinement to particular small areas.

Nam *et al.* [3] have obtained the desired layer via repetition of the process route used to produce the first LEO GaN layer. In this case, the second set of mask stripes were placed directly over the openings of the first LEO mask. This double LEO process required two lithography steps and two depositions of GaN films beyond the growth of the initial seed layer. The process of pendeo-epitaxy (PE) was anticipated to yield the same result—a continuous layer of low defect density GaN—with only one lithography step and a single growth of GaN beyond the seed layer. As its name implies, pendeo-epitaxy is the epitaxial growth of crystalline material that hangs from freestanding forms and is suspended above the substrate. In the particular PE approach used in this research, etched columnar GaN forms were capped with a silicon nitride mask layer. As such, pendeo-epitaxial growth of the GaN films originated only from the sidewalls of these columns. The material grew laterally and vertically until it coalesced between and over the silicon nitride masks located atop the columns in the manner employed in the conventional LEO approach. A continuous layer of low defect density GaN was thus created. This process route was capable of producing continuous layers over large areas and was limited only by the size of the substrate.

B. Experimental Procedure

Pendeo-epitaxial growth of GaN films was performed in the manner shown schematically in Fig. 1.

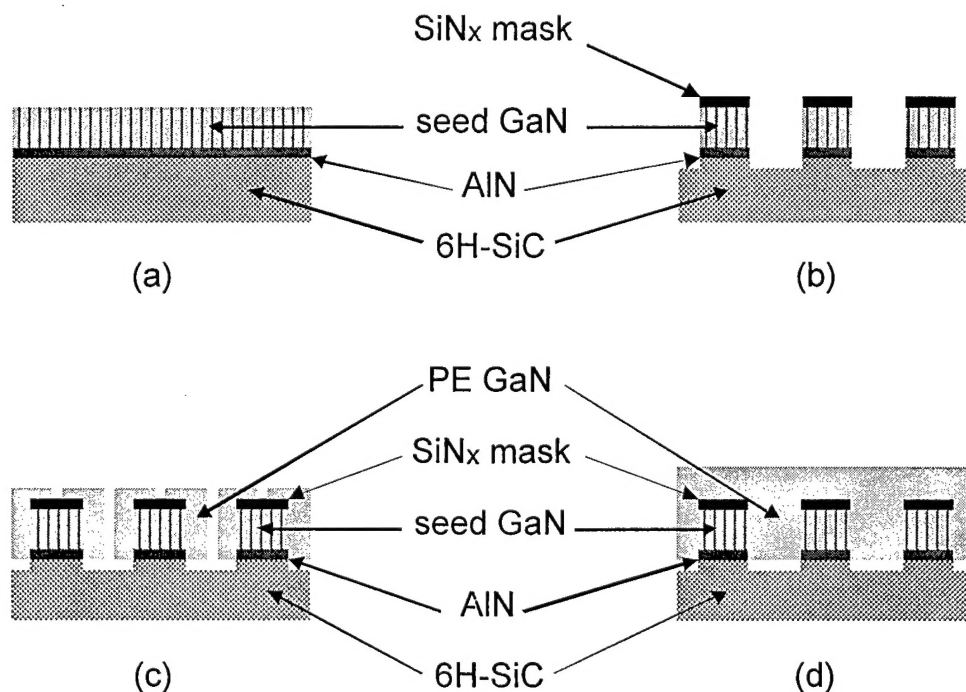


Figure 1. Schematic diagram showing the process steps for growth of pendeo-epitaxial GaN: (a) GaN seed layer, (b) etched GaN columns prior to PE growth, (c) partial growth of PE GaN, (d) coalesced growth of PE GaN.

Each substrate was prepared via growth of a 1 μm thick GaN seed layer at 1000°C on an AlN buffer layer previously grown at 1100°C on a 6H-SiC(0001) substrate in a cold-wall, vertical, pancake-style, RF inductively heated metalorganic vapor phase epitaxy (MOVPE) system. Additional details of the growth experiments have been previously reported [4]. The consecutive deposition of a growth mask layer of silicon nitride (SiN_x) and an etch mask layer of nickel were achieved on the GaN seed layer using plasma enhanced chemical vapor deposition (PECVD) and e-beam evaporation, respectively. The latter mask layer was patterned using standard photolithography techniques in parallel 2 μm wide stripes spaced 3 μm edge-to-edge and oriented along the [1-100] direction of the GaN film. Long columns containing the GaN seed material were produced via inductively coupled plasma (ICP) etching through the SiN_x , GaN and AlN layers and into the 6H-SiC substrate. Detailed procedures for the ICP etching have been previously reported [5]. The nickel etch mask was removed by dipping in HNO_3 for approximately five minutes. The samples were subsequently cleaned by consecutive dips in trichloroethylene, acetone, methanol, and HCl for five minutes each and blown dry with nitrogen.

Pendeo-epitaxial growth of GaN from the (11 $\bar{2}$ 0) sidewalls of the columns was performed at 45 Torr and temperatures ranging from 1000°C to 1100°C via MOVPE. Reactants consisting of 26 $\mu\text{mol/min}$ triethylgallium (TEG) and 1500 sccm ammonia were delivered into the growth chamber and entrained in 3000 sccm of hydrogen diluent. The morphological microstructure of the PE GaN layers was characterized using scanning electron microscopy (SEM-JEOL 6400 FE) in cross-section and plan view. Surface roughness was characterized by atomic force microscopy (AFM-Digital Instruments, Inc. Dimension 3000). Additional modes of PE growth of GaN and $\text{Al}_x\text{Ga}_{1-x}\text{N}$ films and details regarding the procedures employed have been reported externally [6,7] and within this volume [8,9].

C. Results and Discussion

Partially grown GaN pendeo-epitaxy after 30 minutes of growth at 1000°C is shown in Fig. 2(a). No nucleation of the GaN was observed on the surfaces of the etched SiC trenches. The SiN_x mask forced the GaN to grow only from the sidewalls of the etched GaN columns. Growth of the GaN could, therefore, begin only in the lateral directions. As the lateral growth progressed, the GaN began to grow vertically once (0001) top surfaces were created. As the vertical growth reached the top of the mask, lateral growth over the mask commenced. The high lateral to vertical growth ratio (approximately three to one) caused the GaN to wrap around the mask layers.

The results of allowing growth to continue for a total of 80 minutes at 1000°C are shown in Fig. 2(b). Note the presence of the $\sim 60^\circ$ inclined $\{1\bar{1}01\}$ planes, which were the most stable and slowest growing planes in the GaN wurtzite crystal structure [3]. Gaps between the

approaching growth fronts were also observed. These gaps suggested that the growth rates of the laterally growing faces decreased as they came into close proximity. The high vertical growth rates coupled with the continually decreasing space between converging growth fronts resulted in less GaN source material reaching these areas either by surface diffusion or by way of gaseous reactants.

The micrographs shown in Fig. 3 demonstrate the effect of growth temperature on pendeo-epitaxial growth. Figure 3(a) is a plan view of the same film shown in Fig. 2(b), which was grown for 80 minutes at 1000°C.

Coalescence of the GaN was observed in only a few regions. Figure 3(b) is a plan view of PE GaN grown for 80 minutes at 1050°C. The increase in temperature promoted the lateral growth such that the GaN coalesced over much of the surface. Growth for 80 minutes at a

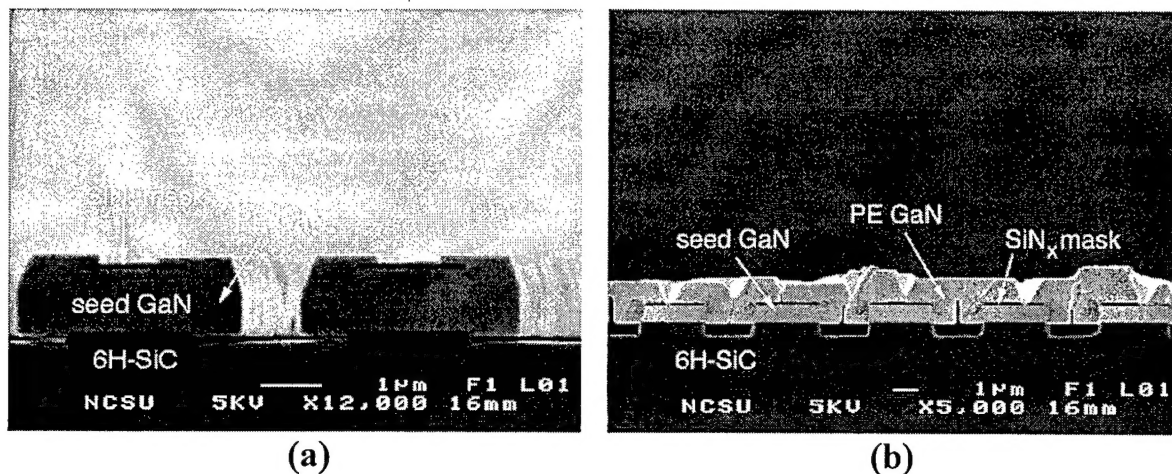


Figure 2. Cross-sectional SEM micrographs of PE GaN grown at 1000°C for (a) 30 minutes, and (b) 80 minutes.

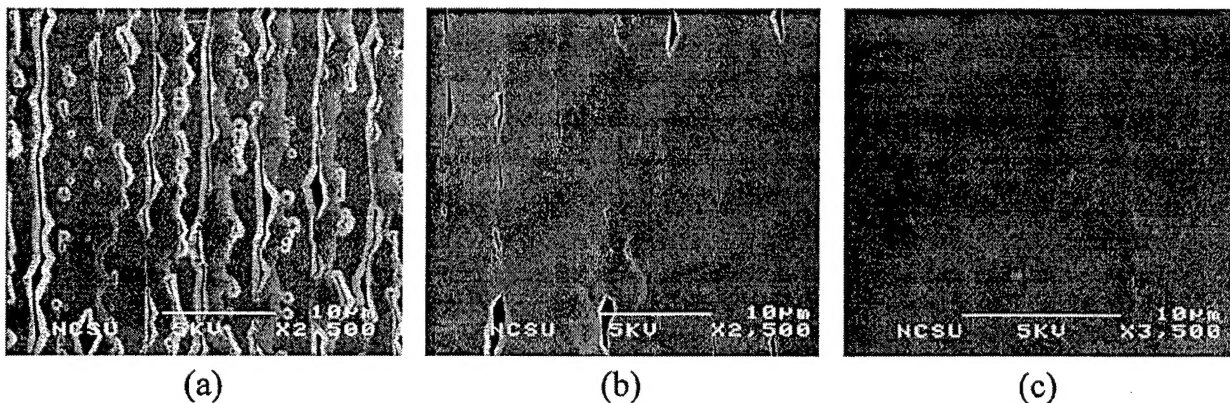


Figure 3. Plan view SEM micrographs of PE GaN grown for 80 minutes at temperatures of: (a) 1000°C, (b) 1050°C, and (c) 1080°C.

temperature of 1080°C resulted in a completely coalesced GaN surface shown in Fig. 3(c). A faint periodicity consistent with the SiN_x stripe spacing was observed. Characterization of this surface using AFM revealed a RMS roughness of 1.32 nm. As the emphasis of the present study focused primarily on determination of parameters necessary for achieving coalescence, optimization of growth parameters subsequent to coalescence was expected to result in smoother PE GaN surfaces suitable for growing device structures.

A cross sectional view of coalesced PE GaN films grown for 80 minutes at 1080°C between and over several columns and masks, respectively, is shown in Fig. 4(a). The origins of the darker areas have not yet been determined. Figure 4(b) is a higher magnification of coalesced PE GaN.

The higher growth temperature promoted swift lateral growth until coalescence was achieved between the columns. As in the LEO approach, the GaN was observed to grow vertically over the edges of the SiN_x mask stripes and laterally across the top until it coalesced with the material growing laterally from the other side of the stripe.

D. Conclusions

Uniform layers of GaN anticipated to have very low dislocation densities over the entire GaN surface have been grown via the technique of pendeo-epitaxy. This process route was an improvement over conventional LEO and was a more efficient method of producing the same results of multiple layers of LEO. Growth temperature was observed to have a significant effect on the morphology of the PE GaN films. Coalescence improved with increasing growth temperatures due to greater lateral to vertical growth ratios. It is expected that pendeo-epitaxy will prove itself useful for improving device quality in optoelectronic and microelectronic applications.

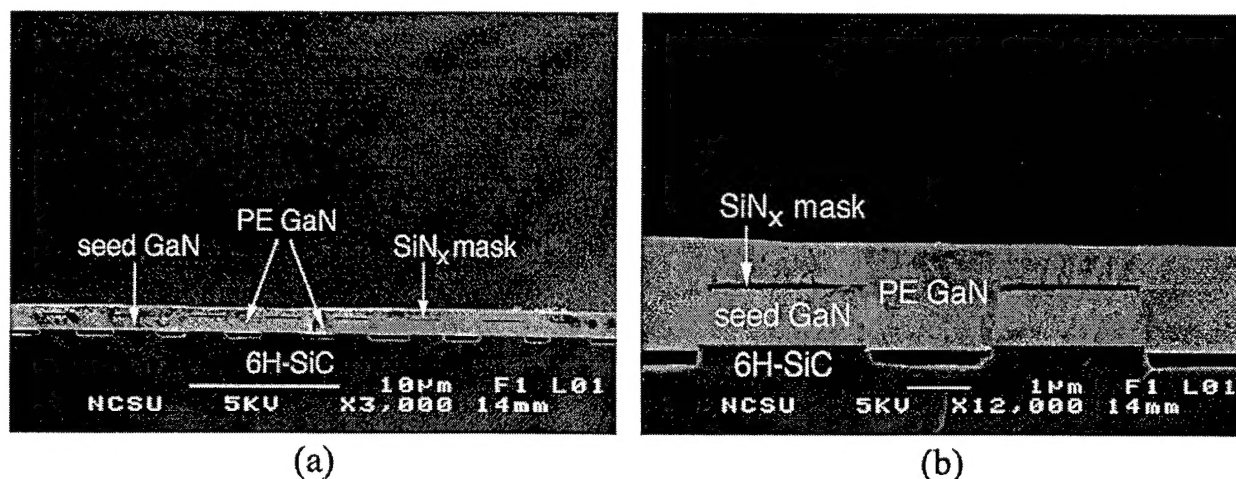


Figure 4. Cross-sectional SEM micrographs of PE GaN grown at 1080°C for 80 minutes showing features at (a) low magnification and (b) high magnification.

E. Acknowledgments

The authors acknowledge Cree Research, Inc. for the SiC wafers. This work was supported by the Office of Naval Research under contracts # N00014-96-1-0765 (Colin Wood, Monitor) and N00014-98-1-0654 (John Zolper, Monitor).

F. References

1. S. Nakamura, The 2nd Intl. Conf. Nitride Semiconductors, Tokushima, Japan, October 25-31, (1997).
2. T. Zheleva, O.H. Nam, J.D. Griffin, M.D. Bremser and R.F. Davis, Mat. Res. Soc. Symp. Proc. **482**, 393 (1998).
3. O.H. Nam, T.S. Zheleva, M.D. Bremser, D.B. Thomson and R.F. Davis, Mat. Res. Soc. Symp. Proc. **482**, 301 (1998).
4. T.W. Weeks Jr., M.D. Bremser, K.S. Ailey, E.P. Carlson, W.G. Perry and R.F. Davis, Jpn. J. Appl. Phys. Lett., **67**, 401 (1995).
5. S.A. Smith, C.A. Wolden, M.D. Bremser, A.D. Hanser, R.F. Davis, and W.V. Lampert, Appl. Phys. Lett. **71**, 3631 (1998).
6. T.S. Zheleva, S.A. Smith, D.B. Thomson, K.J. Linthicum and R.F. Davis, J. Electr. Mat., submitted Nov. 1998.
7. K.J. Linthicum, T. Gehrke, D.B. Thomson, E.P. Carlson, P. Rajagopal, S. Smith and R.F. Davis, Appl. Phys. Lett., submitted Nov. 1998.
8. T. Gehrke, K.J. Linthicum, D.B. Thomson, P. Rajagopal, A.D. Batchelor and R.F. Davis, Mat. Res. Soc. Symp., this volume.
9. K.J. Linthicum, T. Gehrke, D.B. Thomson, K.M. Tracy, E.P. Carlson, S. Smith, T.S. Zheleva and R.F. Davis, Mat. Res. Soc. Symp., this volume.

III. Diluent Gas Effects on Properties of AlN and GaN Thin Films Grown by Metalorganic Vapor Phase Epitaxy on $\alpha(6H)$ -SiC Substrates

A. Hanser, C. Wolden[†], W. Perry, T. Zheleva, E. Carlson, P. Hartlieb, R. F. Davis

Department of Materials Science and Engineering, North Carolina State University, Raleigh, NC 27695

[†]Department of Chemical Engineering, Colorado School of Mines, Golden, CO 80401

Abstract

Thin films of AlN and GaN were deposited on $\alpha(6H)$ -SiC(0001) wafers using metalorganic vapor phase epitaxy (MOVPE) and H₂ and N₂ diluents. A computational fluid dynamic model of the deposition process was used to analyze the film growth conditions for both diluents. Low temperature (12 K) photoluminescence of the GaN films grown in N₂ had peak intensities and full widths at half maximum of ~ 7 meV which were equal to or better than those films grown in H₂. Cross-sectional and plan-view transmission electron microscopy of GaN films grown in both diluents showed similar microstructures with a typical dislocation density of $10^9/\text{cm}^2$. Hall measurements of n-type (Si doped) GaN grown in N₂ revealed Hall mobilities equivalent to those films grown in H₂. Acceptor-type behavior of Mg-doped GaN grown in N₂ was repeatably obtained without post-growth annealing. Secondary ion mass spectrometry revealed equivalent levels of H in Mg-doped GaN films grown in both diluents.

A. Introduction

Blue and green light emitting diodes based on III-Nitrides are commercially available [1], and the fabrication and room temperature continuous wave operation of nitride-based short wavelength injection laser diodes with lifetimes over 10,000 hours have recently been reported [2]. Additionally, microelectronic devices for high-temperature, high-frequency, and high-power applications are being pursued [3,4]. Efforts are ongoing to further improve device performance and to better understand the factors which influence film properties.

In the following sections the results of a computational fluid dynamics model in an inverted MOVPE reactor similar to that used in this research for the growth of III-Nitride materials are presented. The stagnation point flow reactor geometry approximated in our reactor has the

*Presented at the 1997 Fall Meeting of the Materials Research Society, Nitride Semiconductors Symposium, Boston, MA, USA.

potential to produce large area films that are uniform in both thickness and composition [5,6]. Under ideal conditions a flow field is obtained that results in uniform heat and mass transfer gradients across the deposition radius. However, the effects of buoyancy and finite geometries lead to the development of thermal recirculation flows that disrupt the ideal transport conditions. The model results include analysis of the predicted heat and mass transfer gradients and were applied to the deposition of AlN and GaN thin films on SiC substrates. The gas flow structure and the influence of the diluent gas on film properties were investigated. The diluent gas usually constitutes $\geq 50\%$ of the gas phase in the reactor. As such, it essentially helps determine the flow structure in the reactor and often affects the decomposition of the source species. The thermal conductivity and viscosity of the gas phase and the molecular diffusivity of species through this phase are also important in the MOVPE process. H_2 is the primary diluent used in the MOVPE deposition of films of AlN, GaN, and AlGaIn alloys; however, it has been shown to have deleterious effects on the incorporation of In in indium-containing nitride films [7]. The effect of the diluent species, if any, on growth of AlN and GaN are not well known. The influence of H_2 and N_2 diluents on the optical, electrical, and microstructural properties of our AlN and GaN thin films is presented.

B. Experimental Procedures

Computer Modeling. A computational fluid dynamics model was developed using FIDAP, a commercial software package that employs the finite element method, to obtain a better understanding of the factors governing thin film growth in our MOVPE system. The velocity and temperature fields were calculated by solving the following coupled conservation equations in cylindrical coordinates:

$$\nabla(\rho v) = 0 \quad \text{Continuity Equation} \quad (1)$$

$$\rho(v \cdot \nabla v) = -\nabla P + \mu \nabla^2 v + \rho g \quad \text{Conservation of Momentum} \quad (2)$$

$$\rho C_p (v \cdot \nabla T) = \nabla \cdot (k \nabla T) \quad \text{Conservation of Energy} \quad (3)$$

The simplified energy balance neglects contributions from Dufour effects, viscous dissipation, radiation, and heat generated by reactions. Previous work [6, 8] has shown that it is safe to ignore these effects under low pressure MOVPE conditions. The calculations were performed for a binary mixture of ammonia and the diluent gas (H_2 or N_2). The temperature-dependence of the transport properties were abstracted from the Sandia database [9, 10] and included in the simulations. The viscosity and thermal conductivity of the mixture were determined using the semiempirical formula developed by Wilke [11]. It is appropriate to neglect contributions of the metalorganic precursors as they constitute less than 0.01% of the mixture. Buoyancy effects were included in the momentum balance.

The reactor geometry shown in Fig. 1 was simulated in the computer model. The two viewports were excluded to make the system perfectly axisymmetric. The velocity boundary conditions included a zero velocity condition at the inlet and reactor walls. The velocity at the substrate and susceptor were fixed at the rotation speed of 30 RPM. The boundary conditions included neither a radial gradient at the centerline nor an axial gradient at the outlet.

A uniform axial velocity across the gas inlet was assumed. This velocity profile was achieved experimentally following the approach used to generate flat flames for combustion studies [11]. The reactants were first passed through a packed bed to ensure good mixing. A uniform velocity profile was subsequently created by flowing the reactants through a 1-inch long honeycomb structure created by a packed array of thin wall, 1 mm diameter silica tubes. The temperature boundary conditions included in the model were fixed temperatures at the inlet, reactor walls and susceptor and the absence of both a radial gradient at the centerline and an axial gradient at the outlet. A nonuniform mesh employing nine-node biquadratic elements was used to divide the reactor geometry into discrete elements. A typical mesh included ~2000 elements which produced ~20,000 equations and unknowns that were solved using a combination of successive substitution and Newton-Raphson techniques. All calculations were performed at the North Carolina Supercomputing Center.

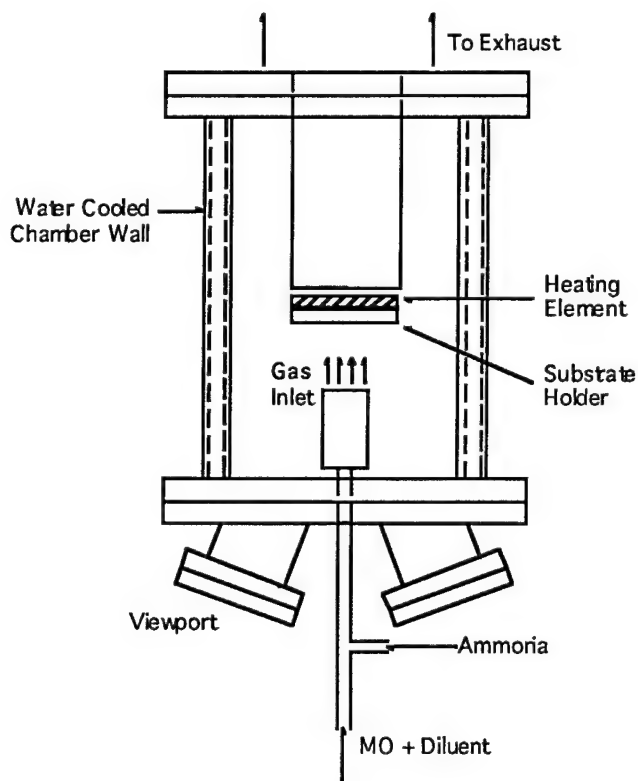


Figure 1. Schematic of the MOVPE deposition chamber.

Film Growth, Doping and Characterization. The AlN and GaN thin films were grown on on-axis 6H-SiC(0001) substrates in an inverted flow, vertical cold wall MOVPE reactor similar to the model described in the previous section and elsewhere [12]. The MOVPE system was operated under computer control using a LabVIEW-based program developed in-house. The substrate was heated to the deposition temperature under a diluent flow of either H₂ or N₂ at 2.2 standard liters per minute (slm). The deposition pressure was 45 Torr. The substrate was rotated continuously at approximately 30 RPM during deposition. Nitrogen was used as the carrier gas for the metalorganic precursors in all depositions. Trimethylaluminum (TMA) and triethylgallium (TEG) were the group III sources, and ammonia (NH₃) was the nitrogen source. The ammonia was delivered to the deposition chamber through a line separate from the metalorganic precursors. Silane (SiH₄) diluted in H₂ was the source for the n-type Si dopant; bis-(cyclopentadienyl) magnesium (Cp₂Mg) was the source for the p-type Mg dopant.

A high-temperature (1100°C) AlN film approximately 1000Å thick was grown directly on each 6H-SiC(0001) substrate as the buffer layer. The GaN deposition conditions were optimized for each diluent. The flow rate of TEG in both diluent gases was 25.0 μmol/min and the flow rate of NH₃ was 1.6 slm. The SiH₄ was introduced into the reactor at flow rates between 0.15 and 3.75 nmol/min; the Cp₂Mg was introduced into the reactor at flow rates between 0.13 and 0.25 μmol/min. After terminating the GaN growth the substrate was cooled at a controlled rate to room temperature under the flowing diluent and NH₃.

The photoluminescence (PL) properties of the films were determined at 12 K using a 15 mW He-Cd laser (λ=325 nm) as the excitation source. Transmission electron microscopy (TEM) was performed at 200 keV using standard sample preparation and imaging techniques. Capacitance-voltage (CV) measurements were made using a mercury (Hg) probe and a computer controlled Hewlett-Packard 4284A LCR meter. Contacts for n-type Hall-effect measurements were made using annealed Ti/Au bilayers; contacts for p-type measurements were made using as-deposited and annealed Ni/Au bilayers. The contacts were deposited on the corners of 7mm × 7mm samples in the Van der Pauw geometry. The contacts were annealed in a RTA system under flowing N₂ at 600 °C for one minute. Hall effect measurements were performed at room temperature. Secondary ion mass spectrometry (SIMS) was conducted using a Cameca IMS-6F system and GaN thin films implanted with H and Mg as standards.

C. Results and Discussion

Figures 2(a) and 2(b) show the calculated velocity contours and temperature contours obtained under the deposition conditions employed for our MOVPE reactor with the use of H₂ and N₂ diluents, respectively. A 60% diluent 40% NH₃ gas mixture was used in the modeling. Figure 2(a) shows the velocity contours for both diluents to be similar, with minimal recirculation cells forming below the substrate. Figure 2(b) demonstrates one of the differences

between the two diluents. The higher thermal diffusivity of H_2 generates higher temperatures further away from the substrate, with a temperature boundary layer approximately 1.5 times as thick as with the N_2 diluent. Uniform temperature gradients are achieved across a majority of the substrate for both diluents. In the mass transport limited regime, the general conclusions can be extended from heat to mass transfer, resulting in predicted uniform transport of the growth species to the substrate across a large area of the substrate. This was experimentally verified using electron microscopy, where a film thickness uniformity variation of $\sim 5\%$ was observed over a 2.54 cm diameter.

The as-grown GaN films had highly reflective surfaces with no visible pits or cracks. A cross-sectional TEM micrograph of a 1 μm GaN film grown in H_2 is shown in Fig. 3. The GaN has a high concentration of defects near the AlN-GaN interface which decreases with distance from the interface. The microstructures of the films grown in both diluents were very similar.

Low temperature (12 K) PL measurements were made on GaN films grown in both diluents. Figure 4 shows the PL spectra for undoped GaN films grown in N_2 diluent. The spectra for films grown in N_2 were characterized by strong near band edge (NBE) emission with a FWHM of 6.90 meV and "yellow" emission levels that were three orders of magnitude lower than the NBE emission. The single feature of the NBE at 358.4 nm (3.460 eV) has been attributed to an exciton bound to a neutral donor (I_2) [13]. The PL spectra for H_2 diluent films were characterized by weaker NBE emission and stronger yellow emission levels, possibly due to non-optimized growth conditions.

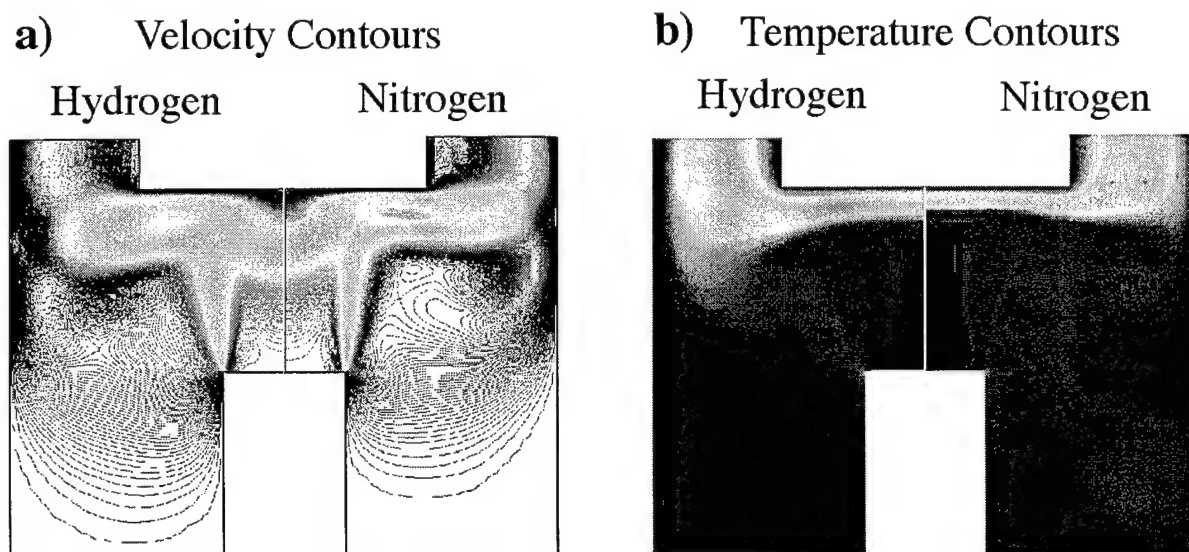


Figure 2. a) velocity contours of the diluent/ NH_3 fluid in the MOVPE reactor under deposition conditions. b) temperature contours of the diluent/ NH_3 mixture under deposition conditions. Conditions for both figures were: $T_{\text{substrate}} = 1000^\circ C$, $P_{\text{system}} = 45$ Torr, T_{inlet} and $T_{\text{wall}} = 25^\circ C$, $V_{\text{inlet}} = 250 \text{ cm} \cdot \text{sec}^{-1}$

Undoped GaN films grown in both H_2 and N_2 were too resistive for Hall measurements. Controlled n-type doping with Si was achieved from $\sim 5 \times 10^{16}$ to $\sim 5 \times 10^{18} \text{ cm}^{-3}$. The maximum room temperature Hall mobility for a $1 \mu\text{m}$ thick film was $275 \text{ cm}^2/\text{V}\cdot\text{s}$ at a carrier concentration of $1 \times 10^{17} \text{ cm}^{-3}$. Magnesium doped GaN films deposited in a nitrogen diluent have repeatably shown p-type behavior as determined by CV measurements without post-growth annealing. All films grown in hydrogen required a post-growth thermal anneal to achieve p-type behavior. Hall measurements on as-grown Mg-doped GaN samples grown in N_2 revealed carrier concentrations as high as $2 \times 10^{17} \text{ cm}^{-3}$ and a Hall mobility of $\sim 13 \text{ cm}^2/\text{V}\cdot\text{s}$. The as-deposited resistivities of these films ranged between $5\text{-}6 \Omega\cdot\text{cm}$.

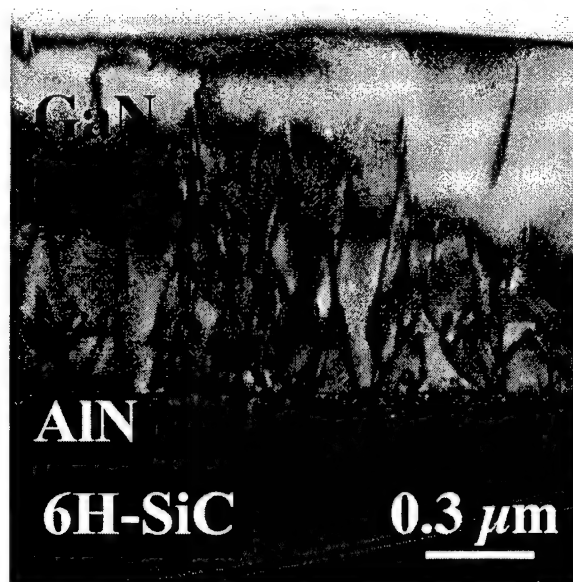


Figure 3. Cross-sectional transmission electron micrograph of a GaN film grown on an AlN buffer layer. Plan view TEM measurements revealed a dislocation density of $\sim 10^9 \text{ cm}^{-2}$.

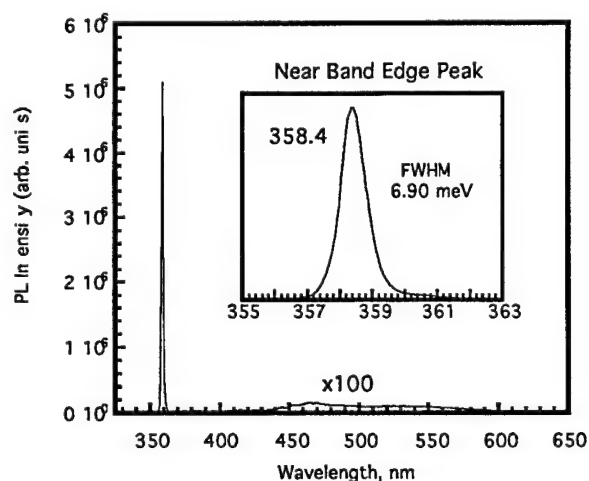


Figure 4. 12 K photoluminescence of GaN grown in a N_2 diluent.

The formation of Mg-H neutral complexes in GaN has been proposed as the passivation mechanism for Mg acceptors [14, 15]. As such, the concentrations of H in undoped and Mg-doped GaN films grown in H_2 and N_2 diluents were investigated using SIMS. Figure 5 shows the H concentration as a function of dopant concentration in Mg-doped GaN films grown in N_2 and H_2 diluents. The H levels for Mg-doped films grown in both diluents were ~ 1.5 to 2 orders of magnitude higher than those in the undoped films. The H level of the film grown in the H_2 diluent was on the order of the H levels in the films grown in the N_2 diluent. Additionally, the H level for the film grown in H_2 was ~ 2 orders of magnitude lower than the Mg level in the film. This would suggest that there is not sufficient H to compensate all the Mg acceptors.

D. Conclusions

Metalorganic vapor phase epitaxy was used to deposit AlN and GaN thin films on on-axis $\alpha(6H)$ -SiC(0001) wafers using H_2 and N_2 diluents. A computational fluid dynamics computer model of the deposition process was employed to analyze the film growth conditions using both diluents. Low temperature (12 K) photoluminescence measurements of GaN films grown in N_2 had peak intensities and full widths at half maximum of ~ 7 meV which was equal to or better than those obtained for films grown in H_2 . Transmission electron microscopy of films grown in both diluents showed similar microstructures. Room temperature Hall measurements of Si doped, n-type GaN grown in N_2 revealed Hall mobilities equivalent to those films grown in H_2 , with a maximum value of $275 \text{ cm}^2/\text{V}\cdot\text{s}$. Acceptor-type behavior of Mg-doped GaN

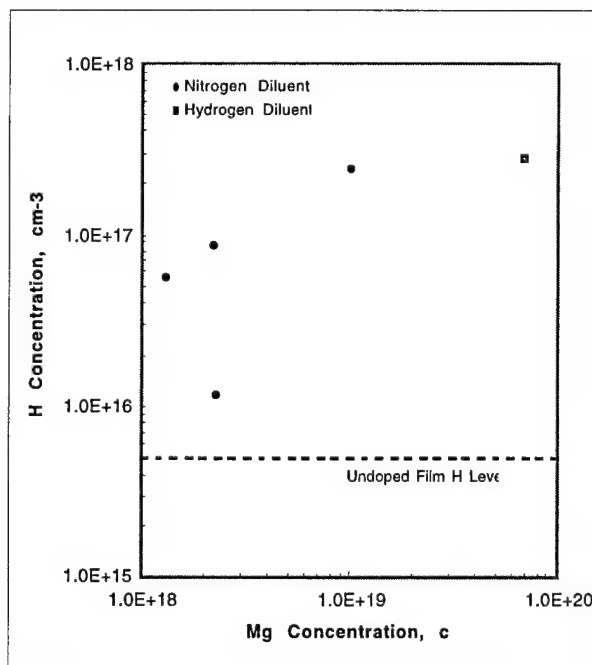


Figure 5. Hydrogen concentration in Mg-doped GaN films vs. magnesium concentration for films grown in N_2 and H_2 diluents.

grown in a N₂ diluent was repeatably obtained without post-growth annealing. Analysis via SIMS of Mg-doped films grown in H₂ and N₂ revealed H concentrations on the same order for both diluents, and ~2 orders of magnitude lower than the Mg doping level in the films.

E. Future Work

Future work include further analysis of the effect of the diluent on the as-grown acceptor-type behavior of Mg-doped GaN thin films. Further SIMS and PL analysis will be employed with rapid thermal annealing studies to obtain an explanation for the acceptor passivation mechanism. Growth of undoped and Si- and Mg-doped Al_xGa_{1-x}N will be examined in both H₂ and N₂ diluents to compare doping ranges as a function of AlN content in the alloy. Gallium nitride and Al_xGa_{1-x}N p-n junction devices, as well as Al_xGa_{1-x}N/GaN MESFET devices will be grown, fabricated and characterized.

F. Acknowledgments

The authors acknowledge the North Carolina Supercomputing Center for providing the computer resources for the modeling work in this paper, and Cree Research, Inc. for providing the SiC wafers. R. Davis was supported in part by the Kobe Steel, Ltd. Professorship.

G. References

1. S. Nakamura, M. Senoh, N. Iwasa, S. Nagahama, *Jpn. J. Appl. Phys.* **34**, L797 (1995).
2. S. Nakamura, 2nd Internat. Conf. on Nitride Semicond. Tokushima, Japan, Oct. 25-31, 1997.
3. Y.-F. Wu, S. Keller, P. Kozodoy, B. P. Keller, P. Parikh, D. Kapolnek, S. P. Denbaars, U. K. Mishra, *IEEE Electron. Dev. Lett.* **18**, 290 (1997).
4. O. Aktas, Z. F. Fan, A. Botchkarev, S. N. Mohammad, M. Roth, T. Jenkins, L. Kehias, H. Morkoç, *IEEE Electron. Dev. Lett.* **18**, 293 (1997).
5. C. Houtman, D. B. Graves, K. F. Jensen, *J. Electrochem. Soc.*, **133**, 961 (1986).
6. G. Evans, R. Grief, *Trans. ASME*, **109**, 928, (1987).
7. E. L. Piner, M. K. Behbehani, N. A. El-Masry, F. G. McIntosh, J. C. Roberts, K. C. Boutros, S. M. Bedair, *Appl. Phys. Lett.* **70**, (4) 461.
8. J. P. Jenkinson, R. Pollard, *J. Electrochem. Soc.* **131**, 2911, (1984).
9. R. J. Kee, F. M. Rupley, J. A. Miller, Sandia National Laboratories Report SAND87-8215, (1994).
10. R. J. Kee, G. Dixon-Lewis, J. Warnatz, M. E. Coltrin, J. A. Miller, Sandia National Laboratories Report SAND86-8246, (1995).
11. C. R. Wilke, *J. Chem. Phys.* **18**, 517 (1950).
12. A. D. Hanser, C. A. Wolden, W. G. Perry, T. Zheleva, E. P. Carlson, A. D. Banks, R. J. Therrien, R. F. Davis, submitted to *J. Electron. Mater.*
13. R. Dingle, D. D. Sell, S. E. Stokowski, M. Ilegems, *Phys. Rev. B* **4**1211 (1971).
14. S. Nakamura, N. Iwasa, M. Senho, T. Mukai, *Jpn. J. Appl. Phys.*, **31** 1258 (1992).
15. W. Götz, N. M. Johnson, J. Walker, D. P. Bour, *Appl. Phys. Lett.*, **67** 2666 (1995).

IV. Electrical Properties of Ni/Au Contacts Deposited on Plasma Treated p-GaN Films Grown Via Organometallic Vapor Phase Epitaxy

A. Introduction

The achievement of p-type conducting GaN has led to the fabrication of such practical devices as blue and green light emitting diodes [1]. The specific contact resistivity of the n-type contact used in these devices has been reported as low as $1 \times 10^{-7} \Omega \cdot \text{cm}^2$ [2]. In contrast, the specific contact resistivity of the p-type contact has only been reported as low as $1 \times 10^{-4} \Omega \cdot \text{cm}^2$ [3], which is far from device quality. Therefore, the thermal stability, as well as the specific contact resistivity of the p-type contact is detrimental to the overall efficiency of GaN-based devices currently being produced and under development [4].

The following report is a detailed account of the behavior of as-deposited Ni/Au contact schemes on pre-treated Mg:GaN films. Identical metallizations were deposited on an untreated Mg-doped GaN thin film, as well as films that were exposed to a 300 W atomic nitrogen plasma at high temperatures.

B. Experimental Procedure

The 1 micron thick Mg-doped GaN films used in this study were grown via OMVPE on a 1200Å thick AlN buffer layer previously deposited at 1100°C on a 6H-SiC substrate. After growth, the GaN films were annealed in an AG Associates 210 rapid thermal annealer at 800°C for 30 seconds. Capacitance voltage (C-V) measurements were made using a Hewlett Packard 4284A C-V measurement system and mercury probe station. Current-voltage measurements were made on the as-deposited contacts using a Keithley 236 Source Measure Unit. Prior to loading, the films were cleaned in subsequent acetone and methanol baths for one minute each, followed by a 10 minute dip in a 1:1 DI:HCl solution. The samples were then immediately loaded into a transfer line operating at a base pressure of 1×10^{-9} Torr.

Two of the three GaN films used in this study were processed in parallel in order to assess the effects of heating and the atomic nitrogen plasma. The net ionized impurity concentrations of these films as measured by C-V were $2 \times 10^{17} \text{ cm}^{-3}$. These films were also treated with an additional 10 second dip in DI water immediately following the DI:HCl solution. The first sample was heated to 470°C, at which point the 300 W plasma was turned on in order to maintain an overpressure of nitrogen so as to prevent the liberation of nitrogen from the surface of the GaN film. Once the sample temperature stabilized at 470°C it was heated to 700°C where it was held for 1 minute and then heated to a temperature of 800°C and held for 10 minutes at a process pressure of 1.4×10^{-4} Torr. The sample was then cooled down to 500°C and the plasma was turned off. The sample was cooled to 200°C whereupon 500Å Ni and 1000Å Au [5] films were deposited using a Hanks HM2 electron beam evaporator operating at a base pressure of

1.7×10^{-9} Torr. The control sample was neither heated nor exposed to the plasma prior to the deposition of an identical metallization at a base pressure of 3.7×10^{-9} Torr. The samples above were patterned using standard photolithographic techniques and etched in a 600 W argon plasma to reveal transfer length method (TLM) patterns whose rectangular pads were 300 μm wide, 1500 μm long and spaced at distances between 5 and 300 μm .

A third film with a net ionized impurity concentration, as measured by C-V, of $7 \times 10^{17} \text{ cm}^{-3}$ was treated in a separate chamber whose base pressure was maintained at 4.7×10^{-7} Torr. The sample was heated to 800°C at which time the 300 W atomic nitrogen plasma was turned on. Once a maximum temperature of 990°C was reached the sample was held at that temperature in the nitrogen plasma for ten minutes at a process pressure of 2×10^{-4} Torr. The sample was then cooled to 800°C at which point the nitrogen plasma was turned off. The sample was cooled to 200°C whereupon it was immediately transferred to the electron beam evaporator and 500Å Ni and 1000Å Au films were deposited at a base pressure of 8×10^{-10} Torr. The metallization was patterned using standard photolithographic techniques and then etched in 1:1:1 $\text{HNO}_3\text{:HCl:DI}$ solution to reveal TLM patterns whose rectangular pads were 300 μm wide, 1500 μm long and spaced at distances between 30 and 300 μm .

C. Results and Discussion

The as-deposited contacts for both the high and low temperature plasma treatments were ohmic (Fig. 1). However, the current-voltage characteristics for the high temperature plasma treatment were considerably better in that the voltage range over which the contacts were ohmic as well as the currents passed were larger than the low-temperature case. Furthermore, the contacts in the high-temperature case yielded a specific contact resistivity of $50 \pm 7 \text{ } \Omega \cdot \text{cm}^2$, while for the low temperature case a specific contact resistivity could not be calculated. This was due to the fact that the low temperature case did not provide consistently ohmic contacts at each pad spacing which is necessary in order to make as accurate TLM calculation [6]. However, the ohmic characteristics of both the high and low temperature plasma treated cases were certainly better than the untreated case (Fig. 2). These improved ohmic characteristics may be attributed to the thermal desorption of Ga at high temperatures, as well as the suppression of nitrogen vacancy formation due to the kinetic effects of nitrogen ions present in the plasma. Ishikawa *et al.* [7] has shown that by sputtering the GaN surface with N ions the N/Ga ratio increases slightly indicating that the formation of nitrogen vacancies is suppressed while the formation of Ga vacancies may be favored. It is postulated that the atomic nitrogen ions in the 300 W plasma may have a similar effect. If this is the case, then the increase in Ga vacancies may decrease the depletion width and increase the tunneling probability, hence leading to favorable ohmic characteristics. This effect could occur on a larger scale in the high temperature case and may account for the results seen here. However, the difference between

the magnitude of net ionized impurities for the samples used in the high and low temperature cases must be taken into account due to the fact that this may overshadow the effects mentioned above.

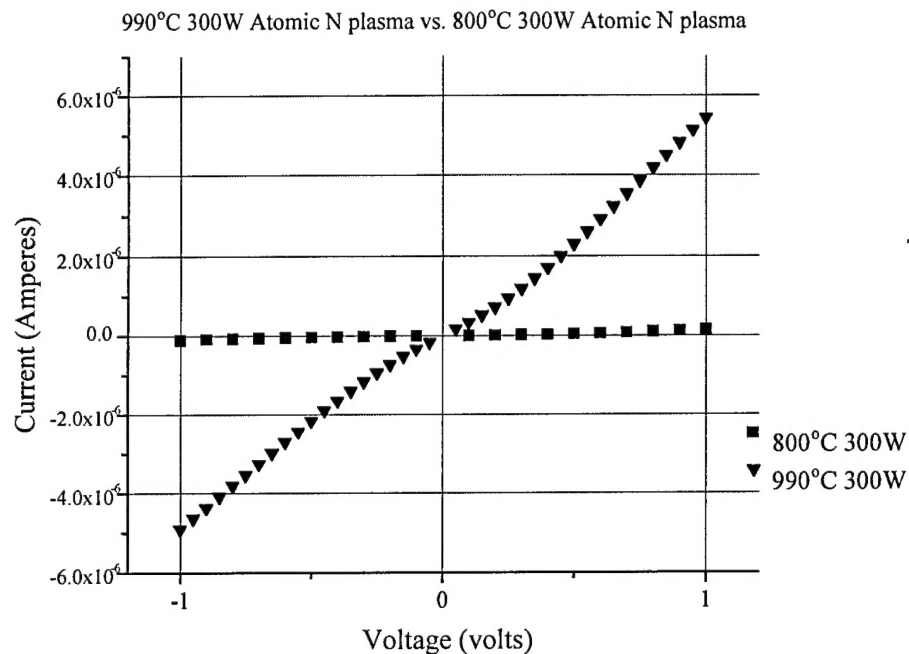


Figure 1. Comparison of Ni/Au contacts on high and low temperature plasma exposed substrates.

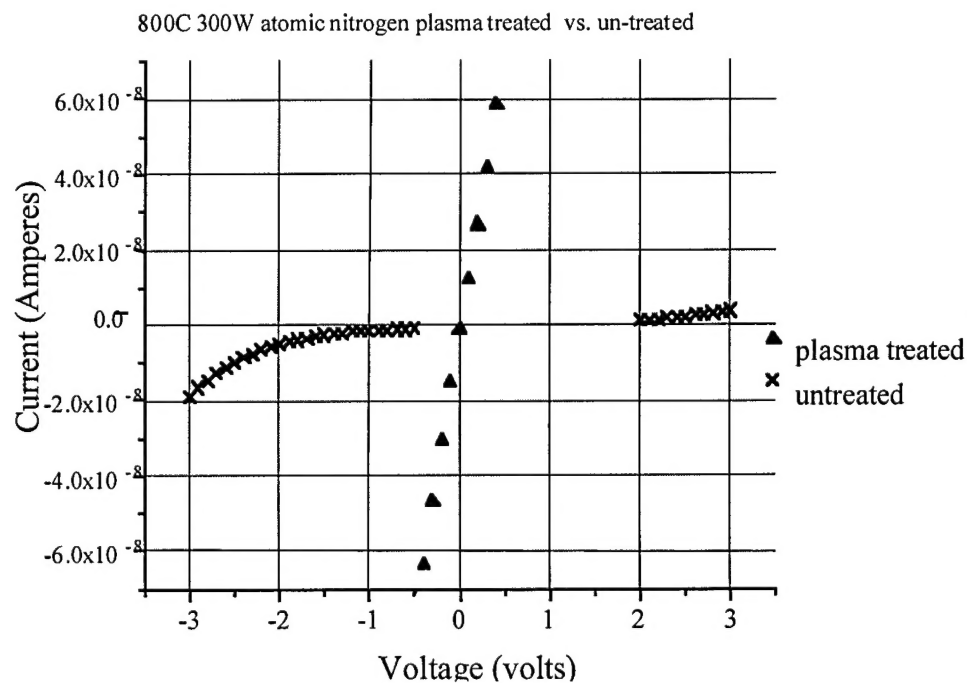


Figure 2. Ni/Au contacts on plasma exposed substrate vs. Ni/Au contacts on an untreated surface.

D. Conclusions

In summary, we have been able to obtain ohmic Ni/Au contacts on plasma treated Mg:GaN in the as-deposited condition with a specific contact resistivity of $50 \pm 7 \text{ } \Omega \cdot \text{cm}^2$. These ohmic characteristics may be attributed to the generation of Ga vacancies at the immediate surface of the Mg:GaN film by atomic nitrogen ions present in the plasma. Future experiments will consider several annealing treatments, as well as alternate metallizations to be used after the plasma pre-treatment.

E. Future Plans and Research Goals

Although it is possible to make ohmic contact to p-GaN [5,8], the specific contact resistivities that have been achieved up until the present time are far from device quality. This is no surprise when one considers the fact that GaN, which has a band gap of $\approx 3.4 \text{ eV}$ and an electron affinity of $\chi \approx 2.7 \text{ eV}$, would require a metal with a work function $\approx 6.1 \text{ eV}$. This certainly presents a problem due to the fact that most metal work functions are never greater than $\approx 5 \text{ eV}$ [9]. Consequently, one is forced into the position of considering a multilevel metallization which would provide an increase in the carrier concentration in the immediate vicinity of the contact or a graded heterostructure in order to achieve a lower specific contact resistivity.

The lowest specific contact resistivity reported to date, which was $\sim 1 \times 10^{-4} \text{ } \Omega \cdot \text{cm}^2$ [3], has been achieved through the use of a solid phase regrowth (SPR) mechanism. This technique has proven to be very effective in forming low resistance ohmic contacts to p type GaAs [11]. "The regrowth process begins with a low temperature reaction between a metal M (e.g. Ni, Pd, or Pt) and a compound semiconductor substrate AB to produce an intermediate M_xAB or MB_x phase. A subsequent reaction at a higher temperature between an overlayer of Si, Ge, Al or In and the intermediate phase results in the decomposition of the intermediate phase and the epitaxial regrowth of a layer of the compound semiconductor [12]." Another vital feature of this mechanism is that the proper dopant be incorporated during the regrowth. This can be achieved by including the appropriate dopant interlayer placed strategically within the metallization so as to optimize the desired thickness of this highly doped regrown layer. This SPR mechanism has also been used to make low resistance ohmic contact to n-GaAs where the final product of the Pd/In/Pd/n-GaAs metallization is PdIn/In_xGa_{1-x}As/n-GaAs/ [12]. Although this graded heterostructure has been used for ohmic contact to n-GaAs no results have been reported regarding its application to GaN.

We plan to use an analogous SPR technique on GaN to grow a In_xGa_{1-x}N/p-GaN heterostructure so as to grade out the large bandgap associated with this material. The metallizations will be as follows Si/Ni/Mg/In/Ni/p-GaN and Si/Ni/In/Mg/Ni/p-GaN. This metallization was chosen due to the fact that Ni has in some cases been shown to form a

NiGaIn ternary phase even at room temperature [11], which is necessary for the first stage of the (SPR) process. At elevated temperatures it is postulated that a NiSi phase is favored to form which would then lead to decomposition of the intermediate phases and regrowth of GaN with In and Mg incorporation. The most formidable obstacles to be overcome in developing this structure will be selecting the appropriate interlayer thicknesses and annealing treatments so as to achieve both Mg and In incorporation in the regrown InGaIn layer. However, the fact that p-type conduction in Mg-InGaIn has been observed [13] is quite encouraging.

The as-deposited and annealed metallizations will be characterized electrically, chemically and microstructurally using transmission line model (TLM) measurements, cross bridge Kelvin resistor (CBKR) measurements, secondary ion mass spectroscopy (SIMS), Auger electron spectroscopy (AES), and high resolution transmission electron microscopy (HRTEM). The interlayer thickness, as well as annealing times and temperatures will then be optimized to give the lowest specific contact resistivity.

F. References

1. S. Nakamura, M. Senoh, N. Iwasa, S. Nagahama, Jpn. J. Appl. Phys. **34**, L797, 1995.
2. Z. Fan, S. Mohammad, W. Kim, O. Aktas, A. Botchkarev, H. Morkoc, Appl. Phys. Lett. **68**, 12, 1996.
3. D. King, L. Zhang, J. Ramer, S. Hersee, L. Lester, Mat. Res. Soc. Symp. Proc. **468**, 421 Pittsburgh, PA, 1997.
4. Y.-F. Wu, S. Keller, P. Kozodoy, B.P. Keller, P. Parikh, D. Kapolnek, S.P. Denbaars, U.K. Mishra, IEEE Electron. Dev. Lett. **18**, 290, 1997.
5. J.T. Trexler, S.J. Miller, P.H. Holloway, M.A. Kahn, Mat. Res. Soc. Symp. Proc. 395 Pittsburgh, PA, 1996.
6. D.K. Schroder, *Semiconductor Material and Device Characterization* (John Wiley and Sons Inc., New York, 1990).
7. H. Ishikawa, S. Kobayashi, Y. Koide, S. Yamasaki, S. Nagai, J. Umezaki, M. Koike, M. Murakami, J. Appl. Phys. **81**, 3, 1997.
8. Taek Kim, Myung C. Yoo, and Taeil Kim, Mat. Res. Soc. Symp. Proc. **449**, Pittsburgh, PA, 1997.
9. D.R. Lide, *Handbook of Chemistry and Physics* (Chemical Rubber, Boston, 1991).
10. E. Kaminska, A. Pitrowska, A. Barcz, L. Ilka, M. Guziewicz, S. Kasjaniuk, E. Dynowska, S. Kwiatkowski, M.D. Bremser, R.F. Davis (unpublished).
11. C.C. Han, X.Z. Wang, L.C. Wang, E.D. Marshall, S.S. Lau, S.A. Schwarz, C.J. Palmstrom, J.P. Harbsison, L.T. Florez, R.M. Potemski, M.A. Tischler, T.F. Kuech, J. Appl. Phys. **68**, 5714 1990.
12. T. Sands, E.D. Marshall, and L.C. Wang, J. Mater. Res. **3**, 914, 1988.
13. S. Yamasaki, S. Asami, N. Shibata, M. Koike, K. Manabe, T. Tanaka, H. Amano, I. Akasaki, Appl. Phys. Lett. **66** (9), 27, 1995.

V. Distribution List

Dr. Colin Wood Office of Naval Research Electronics Division, Code: 312 Ballston Tower One 800 N. Quincy Street Arlington, VA 22217-5660	3
Administrative Contracting Officer Office of Naval Research Atlanta Regional Office 100 Alabama Street, Suite 4R15 Atlanta, GA 30303	1
Director, Naval Research Laboratory ATTN: Code 2627 Washington, DC 20375	1
Defense Technical Information Center 8725 John J. Kingman Road, Suite 0944 Ft. Belvoir, VA 22060-6218	2